Proceedings World Geothermal Congress 2020+1
Reykjavik, Iceland, April - October 2021

Volcanic Texture Identification and Influence on Permeability Using Borehole Resistivity Image Logs in the Taupo Volcanic Zone, New Zealand

Sarah D. Milicich[1], Cécile Massiot[1], David D. McNamara[2], Fabian Sepulveda[3]

[1]GNS Science, 1 Fairway Drive, Avalon, Lower Hutt, 5010, New Zealand

[2]Department of Earth, Ocean and Ecological Sciences, University of Liverpool, UK

[3]Contact Energy Ltd, Wairakei Power Station, Taupo, New Zealand

s.milicich@gns.cri.nz

Keywords: Borehole resistivity image log, Wairakei, permeability, volcanic fabric, New Zealand, fluid flow.

ABSTRACT

Discerning the contributions to fluid flow in a geothermal reservoir from intrinsic and structural permeability components is an important, yet difficult task. High-quality resistivity borehole image log data (Formation MicroImager; FMI) was collected between -669 and -1565 mRL (meters relative to sea level), from a series of lavas, ignimbrites and volcaniclastics in well WK271, Wairakei Geothermal Field, New Zealand. This image log has been used to investigate the textural characteristics of volcanic rocks in the geothermal reservoir, with a view to improving inputs into numerical reservoir models. Textural analysis of the resistivity image log was able to provide a much-improved internal stratigraphy compared to that derived solely from drill-cuttings, revealing the volcanic processes that created the rocks. Several ignimbrite facies, textures inferred to represent volcaniclastic and sedimentary deposition, intervals of breccia, and various rhyolite lava textures are observed and linked to core and outcrop analogues. Based on volcanic textures identified on the WK271 resistivity image log, for the first time we have been able to recognise seven individual flow units in the regionally extensive Whakamaru Group ignimbrite, which are separated by texturally characteristic intervals of airfall tephra, and a high degree of variability and interbedding in the thick Tahorakuri Formation silicic deposits.

Permeability of volcaniclastic formations in geothermal reservoirs is typically controlled by a mixture of fractures and matrix, with some intervals of high density fractures being permeable. There is no clear correlation between rock type and fracture density with most rock types showing variable densities, though non-welded ignimbrites and tuff beds generally have a low fracture density. The textural analysis of this resistivity borehole image log, combined with permeability information from completion test data, thus gives insight into the potential contribution to geothermal fluid flow from intrinsic permeability, along with the volcanic and geothermal processes that formed the geothermal reservoir rocks.

1. INTRODUCTION

Permeability of volcaniclastic formations in geothermal reservoirs is typically controlled by a mixture of fractures and matrix, with the fracture component thought to increase with depth and bulk density (Grant and Bixley, 2011). Characterising the relative contributions of both fracture and matrix permeability throughout a geothermal reservoir is important for field management, reservoir modelling, and future well siting (Bignall et al., 2010).

Borehole image logs are commonly used in geothermal reservoirs as a tool for subsurface structure and stress field characterisation and the identification of where structurally controlled fluid flow occurs in New Zealand (McNamara and Massiot, 2016; McNamara et al., 2017; Massiot et al., 2017a) and overseas (e.g., Genter et al., 1997; Davatzes and Hickman, 2009; Davatzes and Hickman, 2010; Batir et al., 2012). However, borehole image logs can also directly reveal geological formation textures and fabrics, a common practice in petroleum wells (e.g., Watton et al., 2014). In geothermal systems, volcanological interpretation of rocks from borehole image logs is rarely reported (Bartetzko et al., 2003; Davatzes and Hickman, 2005; Halwa et al., 2013; Watton et al., 2014; Massiot et al., 2018; Jerram et al., 2019), with resistivity image logs reportedly advantageous over acoustic image logs for this purpose due to higher contrast of lithological components (Davatzes and Hickman, 2005).

Resistivity image logs are infrequently acquired in New Zealand geothermal wells due to borehole temperatures often exceeding acquisition tool limitations (~175°C). However, when a borehole wall can be cooled to <150°C via quenching, it is possible to acquire resistivity image logs. This practice was first demonstrated in New Zealand in the Ngatamariki Geothermal Field (Halwa et al., 2013), and has only been attempted since in well WK271 in the Wairakei Geothermal Field (Milicich et al., 2018). In this study, we provide observational data on lithological textures and fabrics present throughout geothermal reservoir units in the Wairakei Geothermal Field from the WK271 resistivity image log. Texture, orientation, and layer density are analysed from imaged intervals of the Waiora Formation, Whakamaru Group ignimbrite, Tahorakuri Formation and Karapiti and Kaiapo Rhyolite lavas. From this data insight into depositional processes of the imaged geothermal reservoir units, and the potential intrinsic permeability contribution to geothermal fluid flow are investigated.

1.1 Geological setting

The Wairakei Geothermal Field (348 MWe installed capacity) is located in the Taupo Volcanic Zone (TVZ) in New Zealand (Figure 1), which represents the active, southern portion of the Lau-Havre-Taupo extensional back arc basin, formed as a result of westward subduction of the Pacific Plate beneath the North Island (Begg and Mouslopoulou, 2010; Wilson and Rowland, 2016). The TVZ is the locus of intense silicic volcanic activity during the last ~2 Ma, with multiple ignimbrites sourced from eight calderas (Figure 1; Wilson and Rowland, 2016). The shallow geology (above ~-600 mRL) of the Wairakei area consists of sediments, lavas, and

volcaniclastic deposits <220 ka, and deeper geology consists of a succession of pyroclastic deposits, reworked equivalents, lavas, and sedimentary units (Grindley, 1960; Rosenberg et al., 2009; Bignall et al., 2010). These geological units are variably hydrothermally altered, generally following a trend of increasing rank and intensity with depth (Bignall et al., 2010).

Existing analyses of borehole image data from the Wairakei Geothermal Field, including the well investigated in this study (WK271), indicate that structural (fracture and fault) orientations are dominated by a NE-SW rift-parallel strike, with sub-populations of E-W, and N-S striking structural features (McLean and McNamara, 2011; Massiot et al., 2013; McNamara et al., 2016; Massiot et al., 2017a, McNamara et al., 2019; Massiot et al., 2020).

The Whakamaru Group ignimbrites (Wilson et al., 1986; Brown et al., 1998; Leonard et al., 2010) are a key stratigraphic marker through the TVZ geothermal fields and were erupted in association with collapse of the Whakamaru Caldera (Figure 1) between 349 ± 4 ka to 339 ± 5 ka (Downs et al., 2014). Different flow and fall units have been mapped at the surface and subsurface in several geothermal fields using outcrop and cuttings description complemented by rare cores (Grindley, 1960; Healy et al., 1964; Martin, 1965; Browne, 1971; Briggs, 1976; Leonard et al., 2010; Eastwood et al., 2013), The Tahorakuri Formation, consisting of silicic primary and secondary volcaniclastic rocks, hosts deep geothermal reservoirs, and yet is lithologically poorly defined and constrained as few cores have been recovered, and intense hydrothermal alteration and fine-grained cuttings make differentiation of sub-units challenging (Rosenberg et al., 2009). Both these units have yet to be differentiated using borehole image logging.

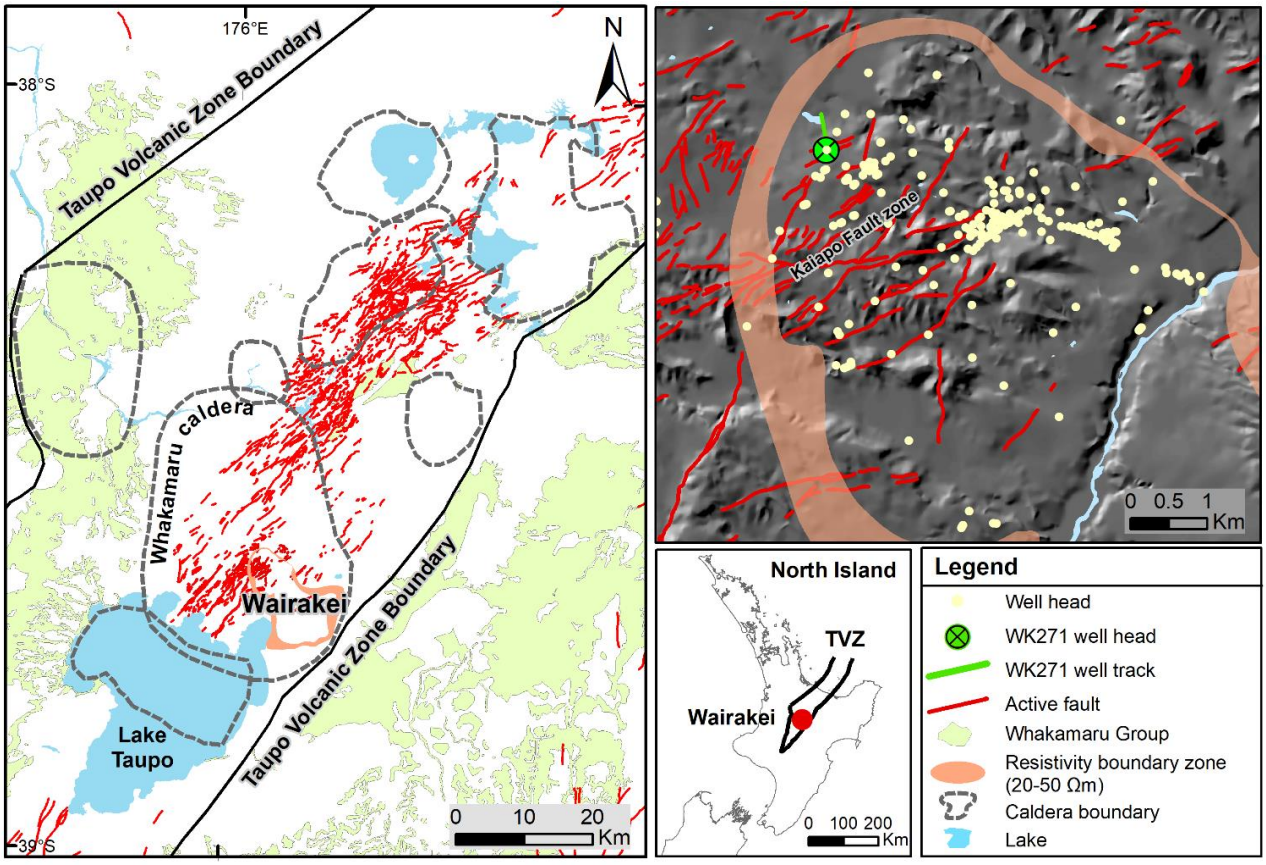

Figure 1: Location of the Wairakei Geothermal Field in relation to the Taupo Volcanic Zone (TVZ; Wilson et al., 1995), caldera boundaries (Wilson et al., 1995), mapped active faults (Langridge et al., 2016) and surface extent of the Whakamaru Group (Leonard et al., 2010). The resistivity boundary of the Wairakei Geothermal Field is delineated by 20-50 Ωm (Risk et al., 1984).

2. DATA AND METHODOLOGY

Well WK271 (Figure 1) was drilled in 2013 to a depth of -1675 mRL (meters with respect to sea level, well head at 520 m above sea level), cased to -670 mRL and deviated ~20° towards NNW (average well inclination 20°, average well azimuth 348°). Resistivity image logs span the entire open-hole section (-674 to -1559 mRL). Resistivity image logs were interpreted following Massiot et al. (2015). The resistivity characteristics of the image are correlated to appropriate core, cuttings, and analogue outcrop descriptions to differentiate lithofacies aspects of the geological units, including presence of lithics, pumice, and dense fracture networks, and internal layering via observation of the overall conductivity appearance of the geological units on the resistivity image log (more resistive = lighter; more conductive = darker). The geological terminology used in this study is schematically summarised in Figure 2. All orientations are with reference to geographic north, and borehole deviation has been taken into account. Texture and layering features were carefully differentiated from natural fractures and stress-induced features.

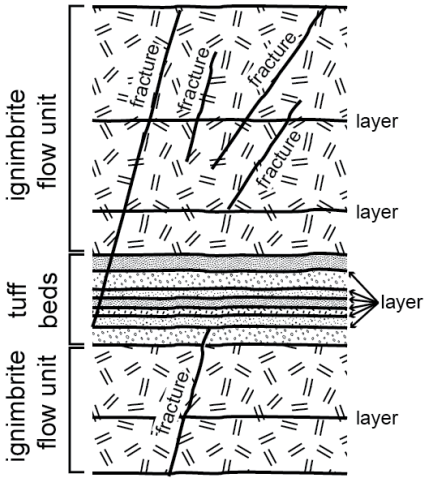

Figure 2: Schematic diagram illustrating geological features and terminology used for interpretation of the resistivity log from well WK271. Pyroclastic rocks consist of beds of ignimbrite with visible layering. Ignimbrite is a volcanic rock formed by widespread deposition and consolidation of ash flows and volcanic ejecta, which includes welded tuff and non-welded but recrystallised/lithified ash flows. "Layer" refers to the internal layering in an ignimbrite or the contact between tuff beds. "Fracture" designates a discordant feature that forms a break in the rock formation.

Interpretation of fractures and stress-induced features is presented in McNamara et al. (2019) and summarised in Massiot et al. (2020). Borehole image logs are presented unwrapped along the north orientation, so that planar features intersecting the cylindrical borehole appear as sinusoids. To account for the under-sampling of sinusoidal features oriented sub-parallel to the borehole, all structural and lithological orientations have been corrected for sampling bias (Terzaghi, 1965; Massiot et al., 2015).

Permeable (feed) zones are interpreted from pressure, temperature and spinner (PTS) completion test data (Massiot et al., 2017a; McNamara et al., 2019).

3. RESULTS: IMAGE ANALYSIS

3.1 Lithological and textural analysis

Textural observations of drill-core from ignimbrite, tuff, rhyolite lava, and volcaniclastic units from the TVZ, or from appropriate outcrop analogues where core is unavailable, are correlated to the resistivity image log responses along well WK271 in order to develop a lithofacies interpretation. Following is a summary of the main lithofacies interpreted from each of the imaged intervals of WK271 drilled formations, with Figure 3 providing some key examples.

Waiora Formation (-726.9 to -936.8 mRL): The imaged interval of the Waiora Formation in WK271 shows distinct blobs of high or low conductivity sitting within the overall lithology. Upon correlation with core, these most likely represent pumice and lithic fragments of varying abundance and size hosted within an ignimbrite matrix (Figure 3.5). Variation in abundance of pumice and lithics and variation in the conductivity of the overall formation (alternating depth intervals of more conductive and more resistive rock) can be observed and correlate to multiple intervals of non-welded ignimbrite as expected from core and cuttings logs of this formation. The base of the Waiora Formation in WK271 is characterised by 3 m of closely spaced layers which have a sharp resistivity contrasts with the underlying Whakamaru Group ignimbrite (Figure 3.8). These closely spaced layers are correlated in core with tuff beds.

Whakamaru Group ignimbrite (-936.8 to -1288.4 mRL): Within the Whakamaru Group ignimbrite, distinct bedding and volcanic textures are visible on the resistivity image log (Figures 3.1 to 3.4, 3.7, 3.9, 3.10). The volcanic textures are interpreted as fiamme (ignimbrite welding texture; Figure 3.2), and breccia (Figure 3.7), along with a range in grain size sorting and degree of sorting. These are consistent with our direct observation of core from Wairakei wells (Figure 3). Some features attributed as layers may be bedding-parallel cooling joints, but cannot be differentiated and have been included as layers. Similar rock fabrics in comparable lithologies have been described from a resistivity image log in the nearby Ngatamariki Geothermal Field (Halwa et al., 2013).

Variations in the rock fabric within the ignimbrite allow it to be subdivided into non-, partially-, and welded ignimbrite. The non-welded zones (Figure 3.1) contain large pumice and lithics which appear as blobs of high or low conductivity. Partially-welded zones (Figures 3.3 & 3.4), similar to the non-welded zones, have pumice of varying sizes, with those < 5 cm showing thickness-width aspect ratios consistent with welding-induced flattening (Bull and McPhie, 2007). Zones of welded ignimbrite (Figure 3.2) have clear fiamme-like (eutaxitic) texture formed from dense, flattened pumice. Ignimbrite flow units are delineated by tuff beds with closely spaced layers (Figure 3.7 & 3.8). There are clear variations in grain size and abundance of both pumice and lithics within the ignimbrite flow units. Along with overall variations, there are also zones of coarse textured breccia (Figure 3.6), which may represent material segregated in the pyroclastic density currents that deposited the ignimbrite (Branney and Kokelaar, 2002). Tuff beds show varying thickness, and in places cross-cutting relationships (Figures 3.5, 3.7 & 3.8).

Tahorakuri Formation (-1288.4 to -1472.5 mRL): The Tahorakuri Formation has a high degree of vertical variability, with multiple changes in lithology observed over distances of <10 m down hole (Figures 3.6, 3.11-12, 3.16). Changes in lithic abundance and size visible in the resistivity image log often mark the change from one ignimbrite unit to another (Figure 3.6). There are intervals with conductive and resistive blobs, interpreted from core to be pumice clasts and lithics in breccia zones (Figure 3.11). There are also intervals of interbedded fine and coarse layers with resistivity contrast between each (Figure 3.12).

Rhyolite lava (-669 to -726.9 mRL and -1472.5 to -1565 mRL): The two rhyolite lavas imaged in WK271 show three main textures on the resistivity image log. 1) The most common texture is massive lava (Figure 3.15), where no internal lava textures are present, though will often be cut by fractures. 2) Flow banding can be seen in some intervals (Figure 3.13), though the resolution of the resistivity image log will not resolve the thinner bands (< 3 mm; FMI resolution is ~5 mm). The flow bands are often not planar (they cannot be fitted with a sinusoid), so have not been included in the layer data. 3) Some intervals of lava are cut by a honeycomb network of fractures (Figure 3.14). Many of the linking fractures in this network cannot be fitted with a sinusoid. Lava textures such as spherulites will usually not be resolved by the resistivity image log, and hence were not identified.

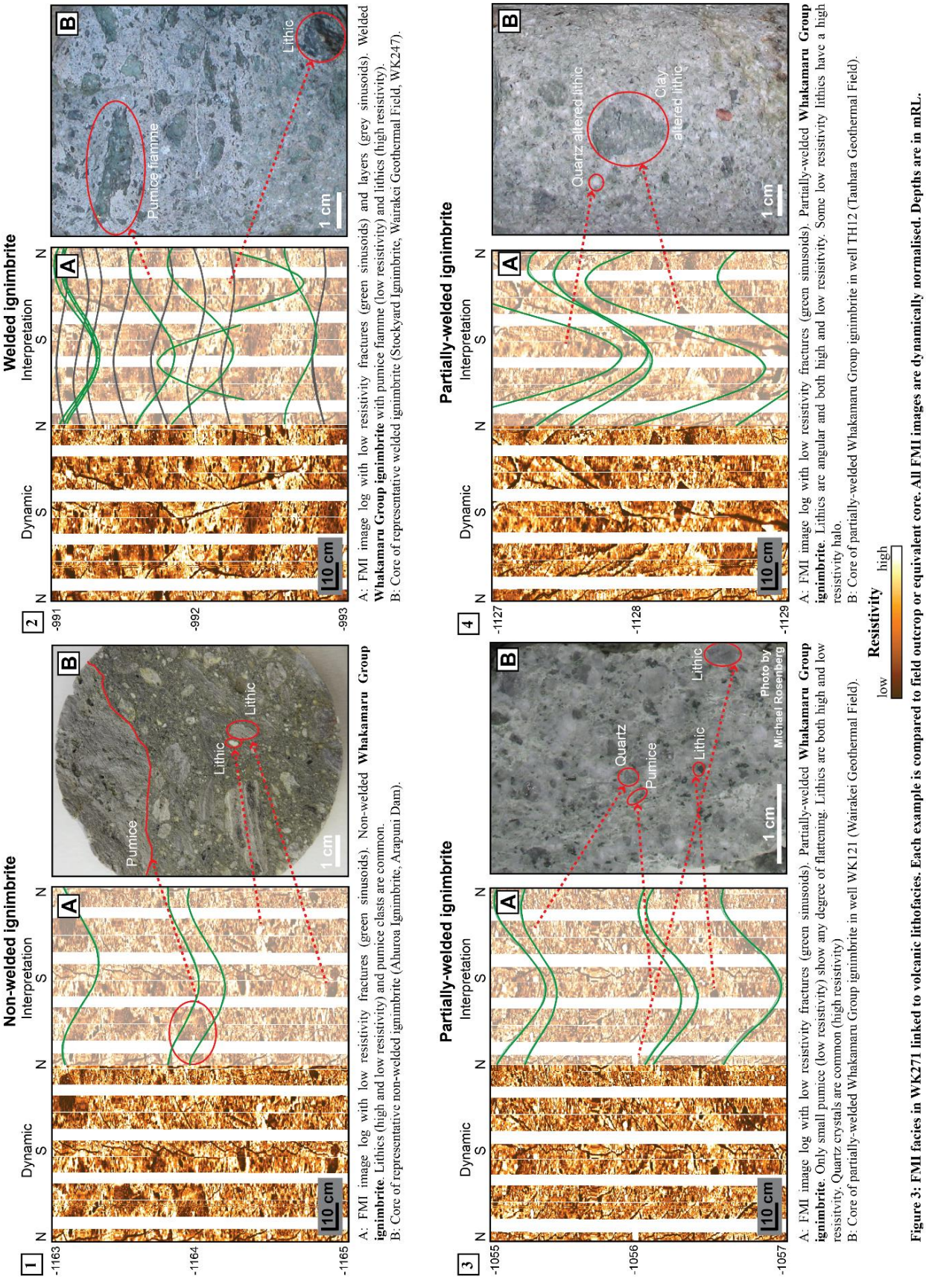

Figure 3: FMI facies in WK271 linked to volcanic lithofacies. Each example is compared to field outcrop or equivalent core. All FMI images are dynamically normalised. Depths are in mRL.

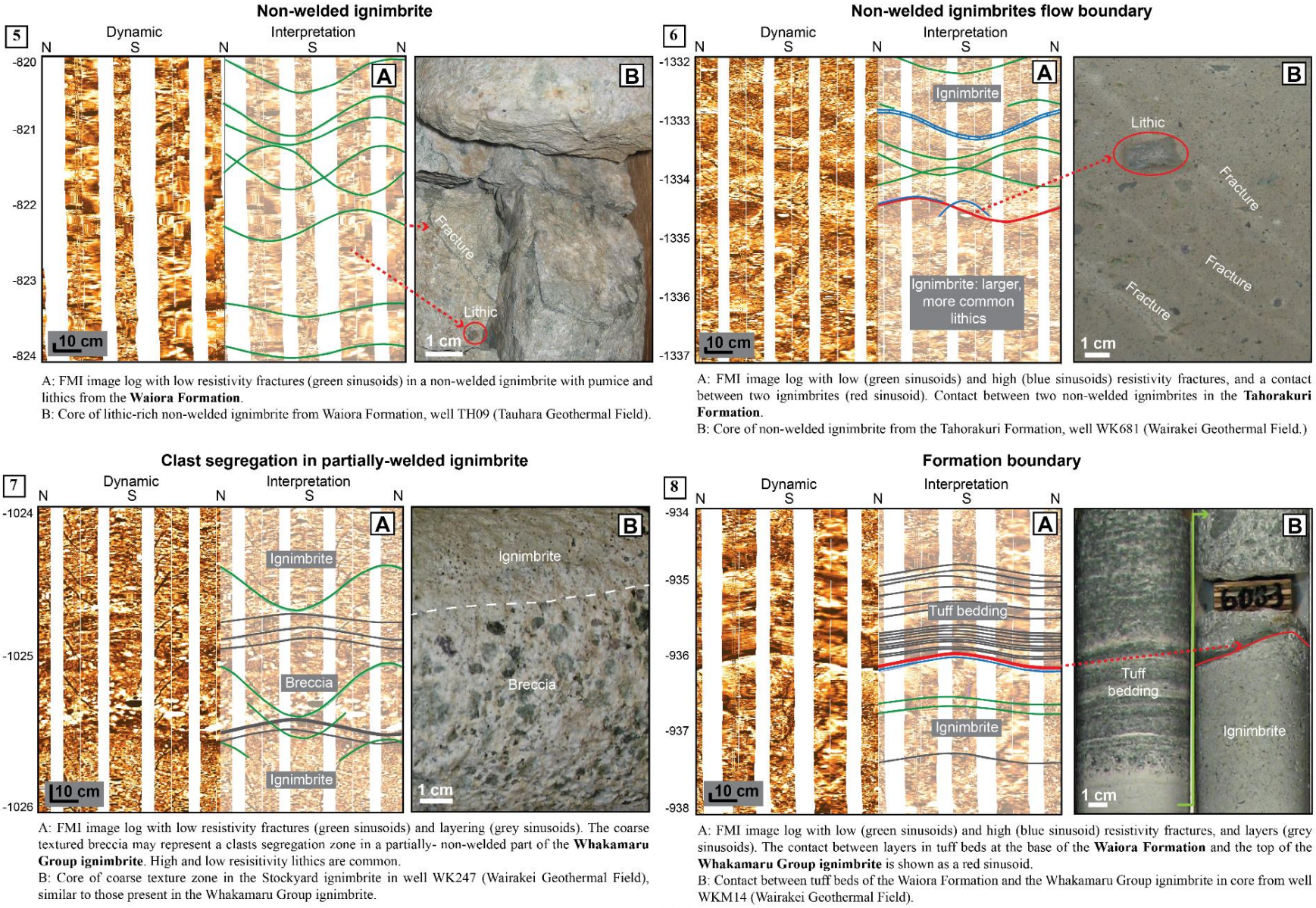

A: FMI image log with low resistivity fractures (green sinusoids) in a non-welded ignimbrite with pumice and lithics from the **Waiora Formation**.
B: Core of lithic-rich non-welded ignimbrite from Waiora Formation, well TH09 (Tauhara Geothermal Field).

A: FMI image log with low (green sinusoids) and high (blue sinusoids) resistivity fractures, and a contact between two ignimbrites (red sinusoid). Contact between two non-welded ignimbrites in the **Tahorakuri Formation**.
B: Core of non-welded ignimbrite from the Tahorakuri Formation, well WK681 (Wairakei Geothermal Field.)

A: FMI image log with low resistivity fractures (green sinusoids) and layering (grey sinusoids). The coarse textured breccia may represent a clasts segregation zone in a partially- non-welded part of the **Whakamaru Group ignimbrite**. High and low resisitivity lithics are common.
B: Core of coarse texture zone in the Stockyard ignimbrite in well WK247 (Wairakei Geothermal Field), similar to those present in the Whakamaru Group ignimbrite.

A: FMI image log with low (green sinusoids) and high (blue sinusoid) resistivity fractures, and layers (grey sinusoids). The contact between layers in tuff beds at the base of the **Waiora Formation** and the top of the **Whakamaru Group ignimbrite** is shown as a red sinusoid.
B: Contact between tuff beds of the Waiora Formation and the Whakamaru Group ignimbrite in core from well WKM14 (Wairakei Geothermal Field).

Figure 3: Continued. All FMI images are dynamically normalised. Depths are in mRL.

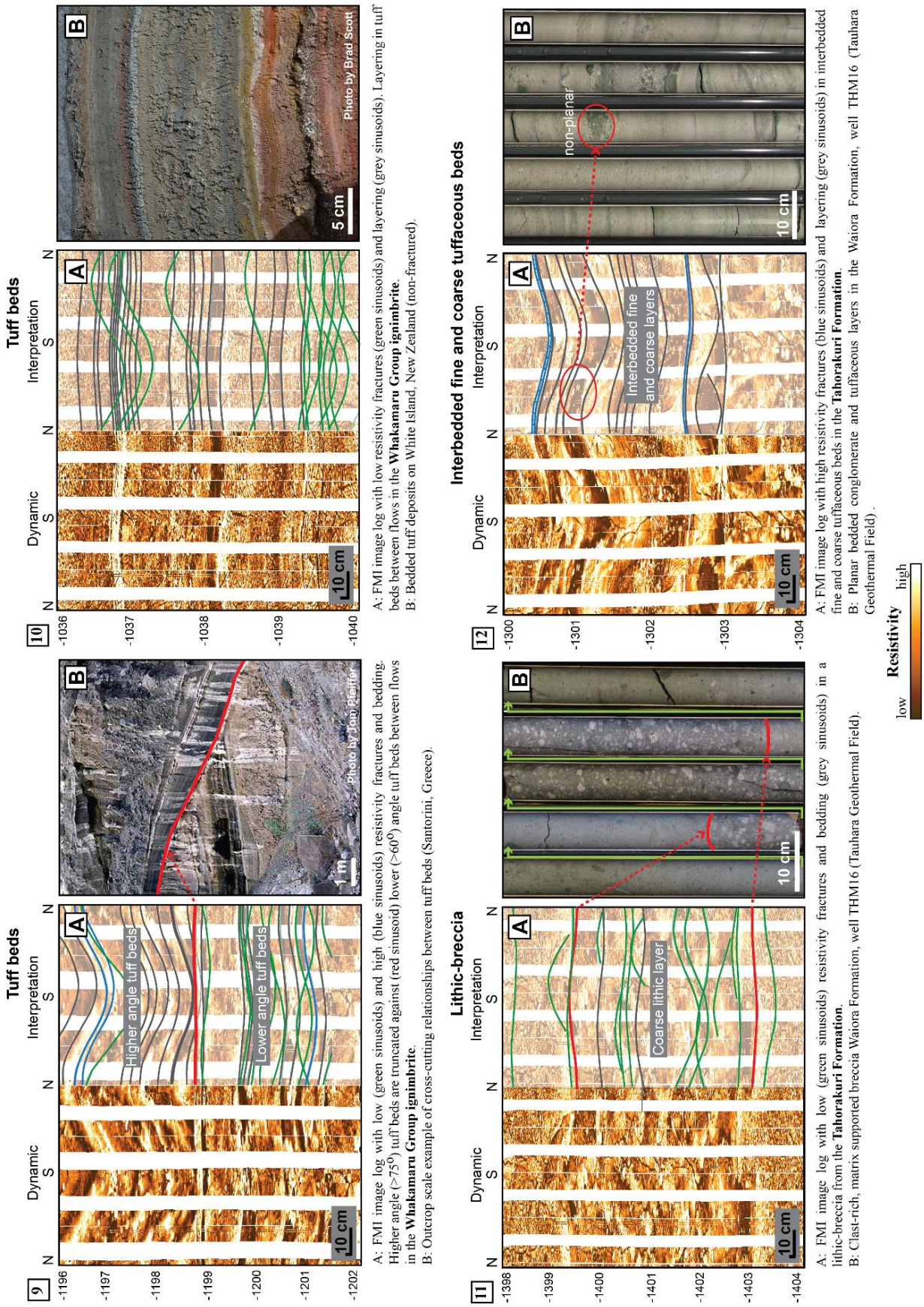

A: FMI image log with low (green sinusoids) and high (blue sinusoids) resistivity fractures and bedding. Higher angle (>75°) tuff beds are truncated against (red sinusoid) lower (>60°) angle tuff beds between flows in the **Whakamaru Group ignimbrite**.
B: Outcrop scale example of cross-cutting relationships between tuff beds (Santorini, Greece).

A: FMI image log with low resistivity fractures (green sinusoids) and layering (grey sinusoids). Layering in tuff beds between flows in the **Whakamaru Group ignimbrite**.
B: Bedded tuff deposits on White Island, New Zealand (non-fractured).

A: FMI image log with low (green sinusoids) resistivity fractures and bedding (grey sinusoids) in a lithic-breccia from the **Tahorakuri Formation**.
B: Clast-rich, matrix supported breccia Waiora Formation, well THM16 (Tauhara Geothermal Field).

A: FMI image log with high resistivity fractures (blue sinusoids) and layering (grey sinusoids) in interbedded fine and coarse tuffaceous beds in the **Tahorakuri Formation**.
B: Planar bedded conglomerate and tuffaceous layers in the Waiora Formation, well THM16 (Tauhara Geothermal Field).

Figure 3: Continued. All FMI images are dynamically normalised. Depths are in mRL.

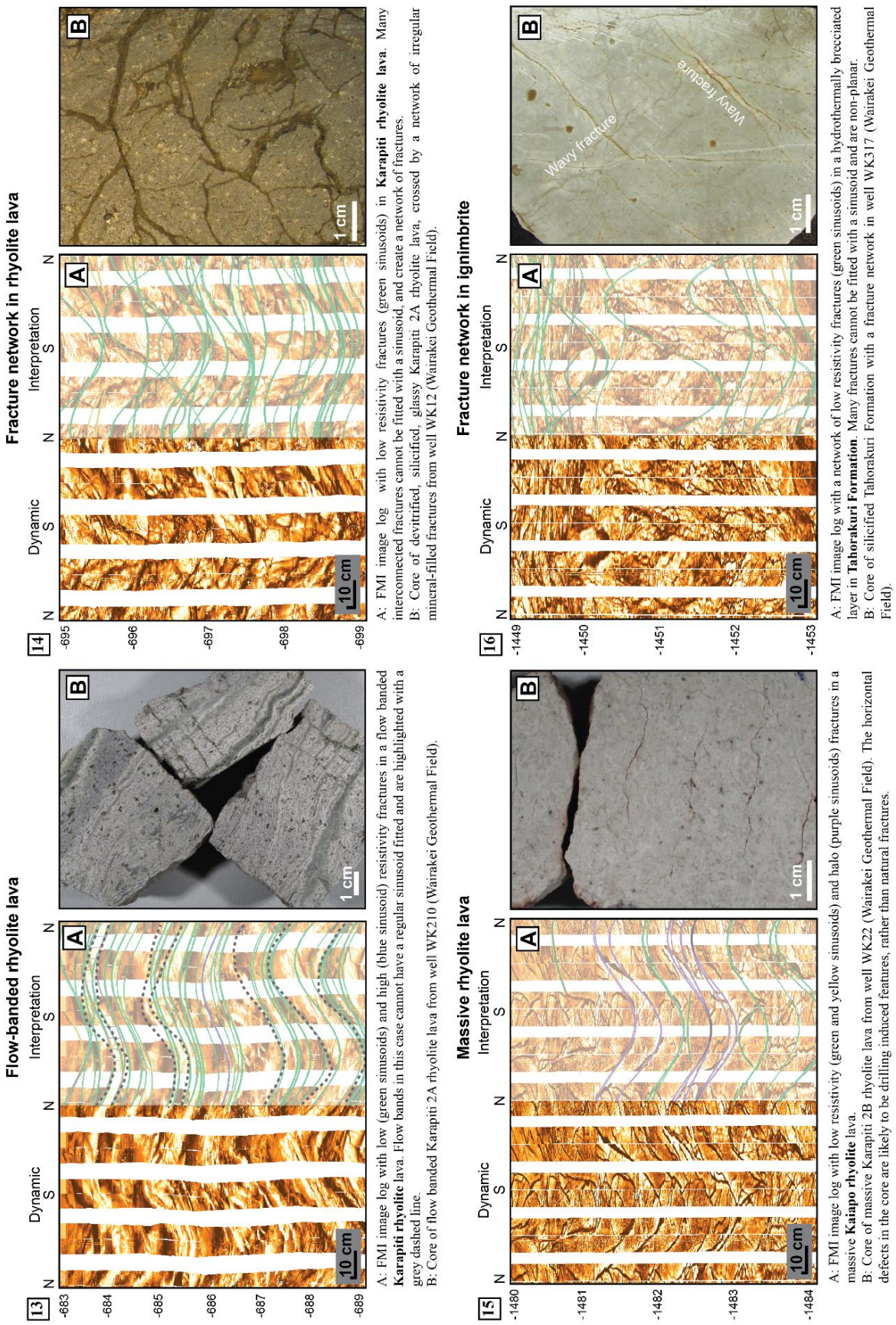

A: FMI image log with low (green sinusoids) and high (blue sinusoid) resistivity fractures in a flow banded **Karapiti rhyolite** lava. Flow bands in this case cannot have a regular sinusoid fitted and are highlighted with a grey dashed line.
B: Core of flow banded Karapiti 2A rhyolite lava from well WK210 (Wairakei Geothermal Field).

A: FMI image log with low resistivity fractures (green sinusoids) in **Karapiti rhyolite lava**. Many interconnected fractures cannot be fitted with a sinusoid, and create a network of fractures.
B: Core of devitrified, silicified, glassy Karapiti 2A rhyolite lava, crossed by a network of irregular mineral-filled fractures from well WK12 (Wairakei Geothermal Field).

A: FMI image log with low resistivity (green and yellow sinusoids) and halo (purple sinusoids) fractures in a massive **Kaiapo rhyolite** lava.
B: Core of massive Karapiti 2B rhyolite lava from well WK22 (Wairakei Geothermal Field). The horizontal defects in the core are likely to be drilling induced features, rather than natural fractures.

A: FMI image log with a network of low resistivity fractures (green sinusoids) in a hydrothermally brecciated layer in **Tahorakuri Formation**. Many fractures cannot be fitted with a sinusoid and are non-planar.
B: Core of silicified Tahorakuri Formation with a fracture network in well WK317 (Wairakei Geothermal Field).

Figure 3: Continued. All FMI images are dynamically normalised. Depths are in mRL.

3.2 Layering orientation

In the imaged interval in WK271 586 geological layers were identified (Figure 4). This does not include non-planar features such as lava flow banding. Of these layers, 303 were identified in the Whakamaru Group ignimbrite, with 82 layers within ignimbrite flow units and 201 layers in bedding intervals between ignimbrite flow units.

Geological layers are predominantly shallow dipping (77% have dip magnitudes ≤40º) to the SW, though there is a subordinate population of steeply dipping layers (5% have dip magnitudes ≥70º, all present in tuff beds from -1181.5 to -1224.8 mRL), dipping to the S (Figure 4). This contrasts with the fractures, which generally dip steeply to the NW and SE (50% have dip magnitudes ≥70º) and confirms the distinction between fractures and layers.

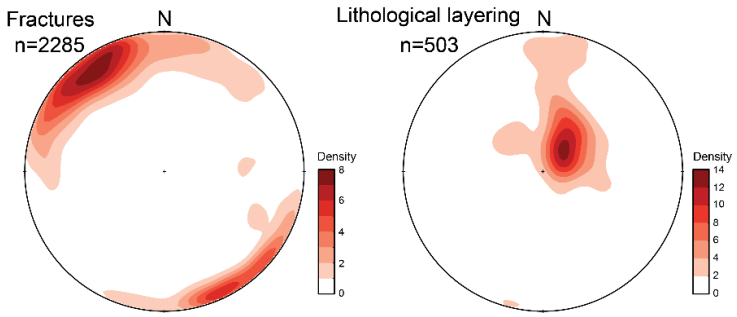

Figure 4: Contoured, lower hemisphere stereonets of poles to planes show fracture (McNamara et al., 2019) and lithological layering orientation for in WK271. Stereonets contoured using Fisher Distribution with color scales representing percentages (Grohmann and Campanha, 2010). Contours are of data corrected for orientation bias; n = raw data set, i.e. uncorrected for orientation bias.

3.3 Layering and fracture density

Layering and fracture density is variable (Figure 5). Fracture density is high in both welded and partially-welded ignimbrite intervals and rhyolite lavas with the lowest density in non-welded ignimbrite and tuff intervals. The highest density of layers occurs in intervals of bedding between ignimbrite flow units.

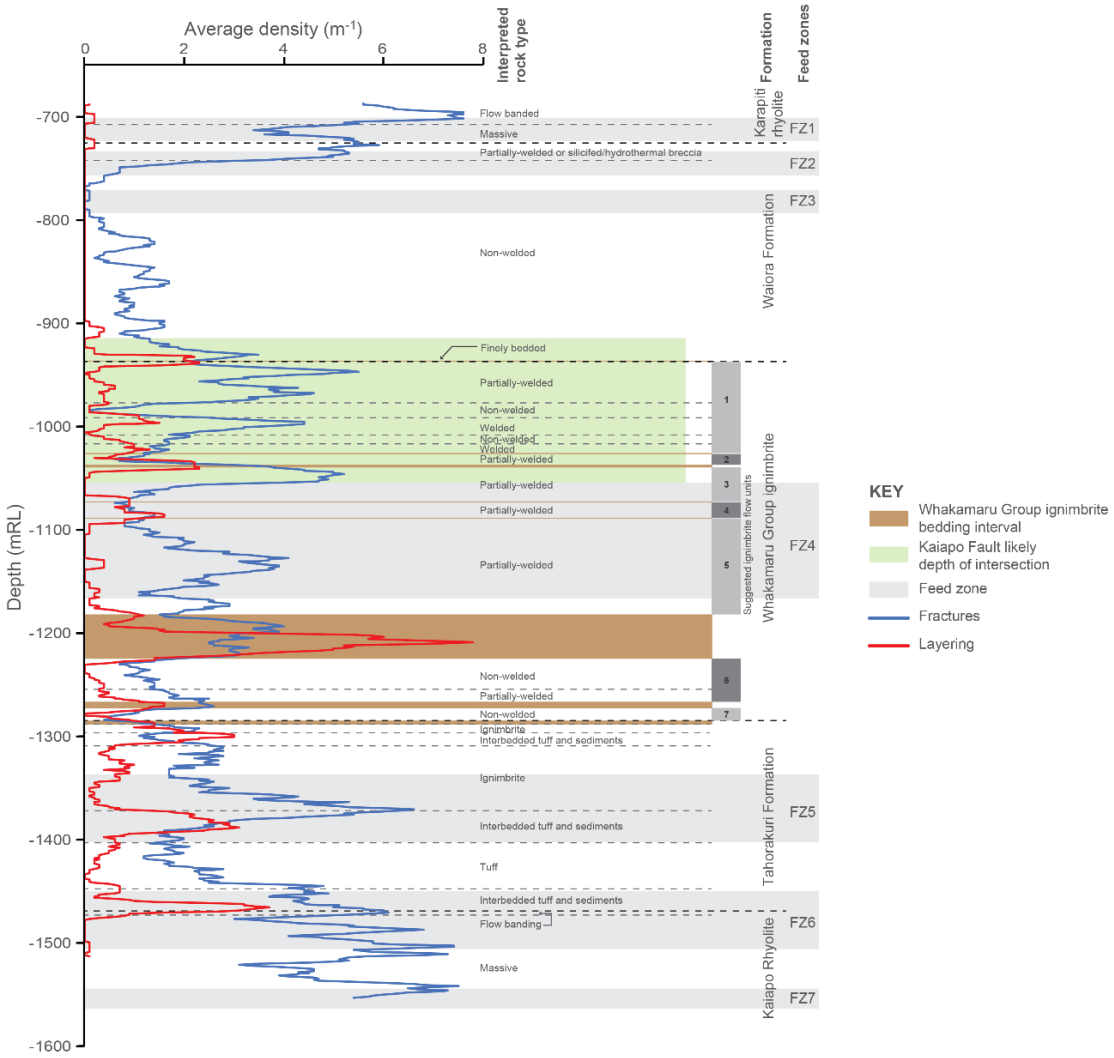

Figure 5: Layering and fracture density (uncorrected for orientation bias) compared to resistivity image log facies in well WK271. The plot was generated with a moving average of fracture and layering data with a window of 10 m and a step of 1 m. The potential intersection of the Kaiapo Fault in the well is indicated, along feed zones identified in Massiot et al. (2017a).

4. DISCUSSION

4.1 Resistivity response of silicic volcanic rocks

Variation in relative resistivity in resistivity image logs can be due to variations in mineralogy, porosity, and fluid content (Galliot et al., 2007). This makes these downhole data well suited to imaging lithological texture and variation in layering or systematic variations in resistivity related to mineralogy or fluids (Davatzes and Hickman, 2005). The dominant resistivity responses of textural and bedding components observed are presented in Table 1.

Table 1: Resistivity response from various volcanic components. "Dark" and "bright" refer to the false-colour scheme used to present the images (Figure 3).

Image component	Dominant alteration mineral	Low resistivity (dark)	High resistivity (bright)
Pumice		✓	
Lithic	Clay	✓	
Lithic	Quartz		✓
Primary quartz			✓
Tuff bed		✓	✓

Hydrothermal alteration minerals can also influence the resistivity response. The imaged interval in well WK271 has a high-temperature alteration assemblage present, with moderate to strong alteration to illite, chlorite, quartz, epidote, pyrite and trace calcite. Of these minerals, clay and quartz are the most abundant and have the highest impact on resistivity response. Clay (both illite and chlorite) will provide low resistivity response and quartz a high resistivity response (Rider, 1996; Halwa et al., 2013). Where lithics are altered to either clays or quartz, they will appear either conductive or resistive with respect to the resistivity response of the surrounding rock (Figure 3.4). Given that quartz is typically associated with a high resistivity response (Halwa et al., 2013), it is likely pumice, given its silicic nature, will also have a high resistivity response. The alteration of pumice to clays could account for the low resistivity response of pumice clasts observed in WK271 (e.g., Figure 3.1). This is consistent with a high degree of clay alteration observed in drill cuttings. Further comparison of core and resistivity image logs, not available to date in the TVZ, would confirm these interpretations.

In addition to the presence of quartz as an alteration mineral, primary volcanic quartz is a common component (>30 vol.%) of the Whakamaru Group ignimbrite and can be characteristically large (up to 5 mm; Leonard et al., 2010). Common, small high resistivity fragments exhibited in some of the imaged intervals (Figure 3.3) may be attributed to these crystals.

The effect of fluid content on resistivity response is likely mixed. Pumice can be porous (high fluid) in non-welded ignimbrite (Figures 3.1, 3.5, 3.6) or relatively non-porous (low fluid) in partially-welded (Figures 3.3, 3.4) to welded ignimbrite (Figure 3.2), but seems to have consistently a low resistivity response. Fluid content appears to have more impact in the resistivity response of tuff beds. These have contrasting high and low resistivity beds, which assuming a relatively consistent mineralogy and componentry, might be due to porosity and hence fluid content variations (Figures 3.5, 3.9, 3.10). It is also possible that variation in grain size would be sufficient to account for the different resistivity response.

4.2 Volcanological implications of intra-formational lithological refinement

Lithofacies analysis of both the Whakamaru Group ignimbrite and Tahorakuri Formation from resistivity image logs in Well WK271 reveals significantly more variation in lithology than use of only drill cuttings (which suggested only one lithology in each). This highlights the advantage of image analysis over drill cutting analysis, where the fine-grained nature, hydrothermal alteration, and mixing of cuttings can obscure the primary rock textures, and centimeter to decimeter volcaniclastic depositional structures and beds. The detailed interpretation of ignimbrite welding intensity in the Whakamaru Group ignimbrite shows that fracture density is low in non-welded intervals (Figure 5). Partial-welded and welded intervals have a higher, but variable fracture density. Low fracture density could be used as an interpretive tool in image logs to identify potential non-welded ignimbrite intervals, where the refinement of welding intensity is not possible from cuttings alone.

The Whakamaru Group ignimbrite is interpreted to have multiple ignimbrite flow units which are delineated by zones of closely spaced layers (Figure 3.9 & 3.10), interpreted as tuff beds formed during short periods of less intense eruptive phases occurring between the emplacement of ignimbrite units. These periods of airfall support the theory that the Whakamaru Group ignimbrite has multiple subdivisions (Briggs, 1976). Using the tuff beds as markers between the larger ignimbrite emplacement events, the Whakamaru Group ignimbrite in this part of the Wairakei Geothermal Field can be divided into at least seven flow units (Figure 5). The 89 m-thick shallowest flow unit could possibly represent several flow units based on variable welding, though as these are not separated by tuff beds, they are not differentiated. The observed truncation of some of these tuff beds on the resistivity image log, and their high angle appearance (Figure 3.9), suggest possible intervals of landscape incision in the times between the ignimbrite forming eruptions and subsequent topographic draping of airfall (McPhie et al., 1993).

Resistivity image log analysis of the Tahorakuri Formation reveals significant lithological variation through the formation, with multiple pyroclastic units (Figures 3.5, 3.6) separated by intervals of bedded layers likely to represent a combination of more minor airfall and sedimentary deposits (Figures 3.11, 3.12). Many of the intervals in the Tahorakuri Formation are likely to be re-sedimented volcanic deposits and distinguishing these from primary airfall will often not be possible. For example, Figure 3.12 shows interbedded fine and coarse layers, which could be either primary or re-worked volcanic deposits. In these intervals, the layering is often non-planar.

Lithofacies in the rhyolite units is more difficult to distinguish from resistivity image logs in well WK271. From geological observations the rhyolite units in the Wairakei Geothermal Field can be massive, flow banded, spherulitic, and brecciated. However, fractures and lithological layer features (such as flow banding) can be challenging to distinguish from each other on a resistivity image logs (Figure 3.13), and spherulites are below the resolution of the tool. In reality, many of the features classified as 'fractures' could also be flow banding, as fractures often follow the pre-existing weaknesses of the flow banding, as seen in Figure 6 in an example from the nearby Rotokawa geothermal system. Fracturing intensity may allow rhyolite flow units to be determined, as heavily fractured 'honeycombed' intervals could be interpreted as breccia tops and bottoms to individual rhyolite flow units, though this is difficult to determine from the image log available from WK271.

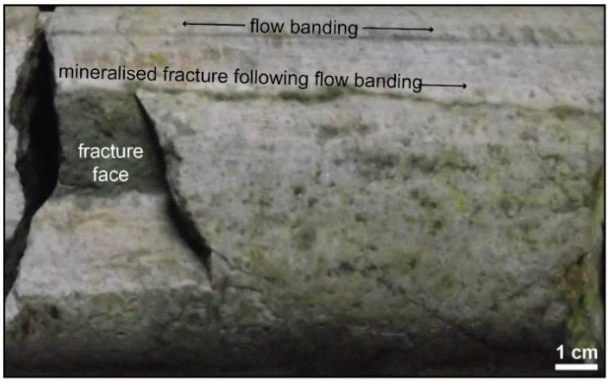

Figure 6: Example of fracturing following flow banding in a rhyolite from the Rotokawa Geothermal Field. After Massiot et al. (2017b).

4.3 Assessment of intrinsic permeability

In well WK271, there is no systematic link between layer density and the feed zones (FZ; Figure 5). The main feed is FZ4, where the density of layers in the feed zone is generally lower that the rest of the Whakamaru Group ignimbrite interval, suggesting that at least in this case, layering in the ignimbrite is not providing significant pathways for fluid flow. The Kaiapo Fault intersects the well WK271 above FZ4 (Figure 5), based on 3D geological modelling (Alcaraz, 2014) utilising stratigraphic offsets and detailed LiDAR surface fault mapping (Villamor et al., 2015). Work by Massiot et al. (2017a) shows that fractures of low resistivity displaying a high resistivity halo (Figure 3.15) are dominantly located within the feed zones. FZ4 contains 43% of all fractures with halo identified in the well, even though this interval covers only 13% of the total imaged well length. Based on the low density of layers in the feed zone, we concur with Massiot et al. (2017a), who suggested that fractures with haloes may be related to the damage zone of the Kaiapo Fault and provide flow pathways. Some of the fluid flow may be controlled by intrinsic permeability and flow along layers, but in this case, the contribution is masked by significant flow associated with fractures (Massiot et al., 2017a). Likewise, in FZ5, these are halo-type fractures, though this FZ also has a peak in fracture density over a change in lithofacies, and lithological layers through an interval of Tahorakuri Formation with high variation in lithofacies. In this case, permeability is likely a combination of intrinsic, fracture and bedding flow.

FZ1, FZ2, FZ6 and FZ7 occur either within a rhyolite lava, or over a formation boundary with the rhyolite lava. These feed zones have a high density of fractures, but also flow banding and brecciation in the rhyolite lava, suggesting permeability is related to a combination of lithological and structural controls.

FZ3, located within a non-welded ignimbrite, is the only feed zone where intrinsic permeability is likely the main source of permeability, as it has few layers and fractures.

5. CONCLUSIONS

The resistivity image log interpretation of well WK271 in the Wairakei Geothermal Field allows a high-resolution investigation of volcanic textures within geological units that were previously unknown. The resistivity image log textural interpretation improves resolution of the stratigraphic sequence, unable to be determined by examination of drill cuttings. This has provided additional insight into the volcanic products of one of the large caldera forming Whakamaru Group eruptive sequences in the TVZ, with the identification of at least seven discrete flow units, separated by fine-grained layers thought to represent short-lived, less-intense, eruptive phases.

Analysis of resistivity image log in well WK271 confirms that fluid flow is dominantly contributed through fractures and fault damage zones, with in places contribution from flow through geological layers and intrinsic permeability. The detailed analysis of lithofacies and fractures from resistivity image logs, beyond that capable by interpretation of drill cuttings, combined with PTS is required to fully understand the nature of individual feed zones.

Volcanological, textural, and lithological interpretation from resistivity image logs, in addition to the usual structural interpretations, are proven here to be critical inputs into improving resolution of 3D geological, conceptual and numerical models of a geothermal system, and stand to improve well targeting and reservoir management.

ACKNOWLEDGEMENTS

This study is part of GNS Science's *New Zealand Geothermal Future* research programme, funding of which was provided by the Government of New Zealand. We thank Contact Energy Ltd. for the provision and permission to publish well data. The authors acknowledge support of this work by Haliburton Software and Services, a Haliburton Company, through the use of Recall™ Borehole software. Thanks to Mark Lawrence, and Michael Rosenberg for valuable discussion and editorial comments.

REFERENCES

Alcaraz, S.A.: Update to the Wairakei-Tauhara 3-D geological model. GNS Science consultancy report 2014/113LR (2014).

Bartetzko, A., Paulick, H., Iturrino, G., Arnold, J.: Facies reconstruction of a hydrothermally altered dacite extrusive sequence: evidence from geophysical downhole logging data (ODP Leg 193). *Geochemistry, Geophysics, Geosystems*, (2003), 4.

Batir, J., Davatzes, N.C.: Preliminary model of fracture and stress state in the Hellisheidi Geothermal Field, Hengill Volcanic System, Iceland. Proceedings, 37th Workshop on Geothermal Reservoir Engineering, Stanford University, Stanford, CA (2012).

Begg, J.G., Mouslopoulou, V.: Analysis of late Holocene faulting within an active rift using lidar, Taupo Rift, New Zealand. *Journal of Volcanology and Geothermal Research*, 190, (2010), 152-167.

Bignall, G., Milicich, S.D., Ramirez, L E., Rosenberg, M.D., Kilgour, G.N., Rae, A. J.: Geology of the Wairakei-Tauhara geothermal system, New Zealand. Proceedings, Worlds Geothermal Congress, Bali, Indonesia (2010).

Bignall, G., Rae, A., Rosenberg, M.: Rationale for targeting fault versus formation-hosted permeability in high-temperature geothermal systems of the Taupo Volcanic Zone, New Zealand. Proceedings, World Geothermal Congress, Bali, Indonesia (2010).

Branney, M.J., Kokelaar, B.P.: Pyroclastic density currents and the sedimentation of ignimbrites. Geological Society of London, (2002).

Briggs, N.D.: Recognition and correlation of subdivisions within the Whakamaru Ignimbrite, central North Island, New Zealand. *New Zealand Journal of Geology and Geophysics*, 19, (1976), 463-501.

Brown, S.J.A., Wilson, C.J.N., Cole, J.W., Wooden, J.: The Whakamaru group ignimbrites, Taupo Volcanic Zone, New Zealand: evidence for reverse tapping of a zoned silicic magmatic system. *Journal of Volcanology and Geothermal Research*, 84, (1998), 1-37.

Browne, P.R.L.: Petrological logs of drillholes, Broadlands geothermal field. New Zealand Geological Survey, Report 52 Lower Hutt (1971).

Bull, K.F., McPhie, J.: Fiamme textures in volcanic successions: Flaming issues of definition and interpretation. *Journal of Volcanology and Geothermal Research*, 164, (2007), 205-216.

Davatzes, N.C., and Hickman, S.H.: Comparison of acoustic and electrical image logs from the Coso geothermal field, CA. Proceedings, 30th Workshop on Geothermal Reservoir Engineering, Stanford University, Stanford, CA (2005).

Davatzes, N. C., Hickman, S.H. (2009). Fractures, stress and fluid flow prior to stimulation of well 27-15, Desert Peak, Nevada, EGS Project. Proceedings, 34th Workshop on Geothermal Reservoir Engineering, Stanford University, Stanford, CA (2009).

Davatzes, N., Hickman, S.H.: Stress, fracture, and fluid-flow analysis using acoustic and electrical image logs in hot fractured granites of the Coso geothermal field, California, U.S.A. In M. Pöppelreiter, Garcia-Carballido and Kraaijveld (eds.), Dipmeter and Borehole Image Log Technology, American Association of Petroleum Geologists Memoir 92, Tulsa OK, 259-294 (2010).

Downs, D.T., Rowland, J.V., Wilson, C.J.N., Rosenberg, M.D., Leonard, G.S., Calvert, A.T.: Evolution of the intra-arc Taupo-Reporoa Basin within the Taupo Volcanic Zone of New Zealand. *Geosphere*, 10, (2014), 185-206.

Eastwood, A.A., Gravley, D.M., Wilson, C.J.N., Chambefort, I., Oze, C., Cole, J.W., Ireland, T.R.: U-Pb dating of subsurface pyroclastic deposits (Tahorakuri Formation) at Ngatamariki and Rotokawa geothermal fields, Proceedings, 35th New Zealand Geothermal Workshop, Rotorua, New Zealand (2013).

Galliot, P., Brewer, T., Pezard, P., Yeh, E.: Borehole imaging tools – principles and applications. *Scientific Drilling*, 5, (2007), 1-4.

Genter, A., Traineau, H., Dezayes, C., Elsass, P., Ledesert, B., Meunier, A., Villemin, T.: Fracture analysis and reservoir characterization of the granitic basement in the HDR Soultz Project (France). *Geothermal Science and Technology*, 4, (1995), 189–214.

Grant, M.A., Bixley, P.F.: Geothermal Reservoir Engineering (2nd ed.). Burlington, USA: Academic Press (2011).

Grindley, G.W.: Sheet 8—Taupo. Geological map of New Zealand 1: 250 000. Department of Scientific and Industrial Research, Wellington, New Zealand (1960).

Grohmann, C.H., Campanha, G.A.C.: OpenStereo: Open source, cross-platform software for structural geology analysis. Abstract IN31C-06 presented at 2010 Fall Meeting, AGU, San Francisco, California (2010).

Halwa, L., Wallis, I.C., Lozada, G.T.: Geological analysis of the volcanic subsurface using borehole resistivity images in the Ngatamariki Geothermal Field, New Zealand. Proceedings, 35th New Zealand Geothermal Workshop (2013).

Healy, J., Schofield, J.C., Thompson, B.N.: Geological map of New Zealand 1:250,000 Sheet 5 Rotorua. Department of Scientific and Industrial Research, Wellington, New Zealand (1964).

Hurley, N.F.: Recognition of faults, unconformities, and sequence boundaries using cumulative dip plots. *American Association of Petroleum Geologists Bulletin*, 78, (1994), 1173-1185.

Jerram, D.A., Millett, J.M., Kück, J., Thomas, D., Planke, S., Haskins, E., Lautze, N., Pierdominici, S.: Understanding volcanic facies in the subsurface: a combined core, wireline logging and image log data set from the PTA2 and KMA1 boreholes, Big Island, Hawaii. *Scientific Drilling*, 25, (2019), 15-33.

Langridge, R.M., Ries, W.F., Litchfield, N.J., Villamor, P., Van Dissen, R.J., Barrell, D., Langridge R.M., Rattenbury, M.S., Heron, D.W., Haubrock, S., Townsend, D.B., Lee, J.M.: The New Zealand active faults database. *New Zealand Journal of Geology and Geophysics*, 59, (2016), 86–96.

Leonard, G.S., Begg, J.G., Wilson, C.J.N. (compilers): Geology of the Rotorua area: scale 1:250,000. Institute of Geological & Nuclear Sciences Limited, Lower Hutt, New Zealand (2010).

Lofts, J.C., Bourke, L.T.: The recognition of artefacts from acoustic and resistivity borehole imaging devices. *Geological Society, London, Special Publications*, 159, (1999), 59–76.

Martin, R.C.: Lithology and eruptive history of the Whakamaru ignimbrites in the Maraetai area of the Taupo volcanic zone, New Zealand. *New Zealand Journal of Geology and Geophysics*, 8, (1965), 680-705.

Massiot, C., McNamara, D.D., Lewis, B.: Interpretive review of the acoustic borehole image logs acquired to date in the Wairakei-Tauhara Geothermal Field. GNS Science report 2013/04 (2013).

Massiot, C., McNamara, D.D., Lewis, B.: Processing and analysis of high temperature geothermal acoustic borehole image logs, New Zealand. *Geothermics*, 53, (2015), 190–201.

Massiot, C., McLean, K., McNamara, D.D., Sepulveda, F., Milicich, S.D.: Discussion between a reservoir engineer and a geologist: permeability identification from completion test data and borehole image logs integration. Proceedings, 39th New Zealand Geothermal Workshop, Rotorua, New Zealand (2017a).

Massiot, C., Nicol, A., McNamara, D.D., Townend, J.: Evidence for tectonic and thermal controls on fracture system geometries in an andesitic high-temperature geothermal field. *Journal of Geophysical Research: Solid Earth*, (2017b), 122.

Massiot, C., Célérier, B., Doan, M.-L., Little, T. A., Townend, J., McNamara, D. D., Williams, J., Schmitt, D.R., Toy, V.G., Sutherland, R., Janku-Capova, L., Upton, P., Pezard, P. A.: The Alpine Fault Hangingwall Viewed From Within: Structural Analysis of Ultrasonic Image Logs in the DFDP-2B Borehole, New Zealand. *Geochemistry, Geophysics, Geosystems*, 19, (2018), 2492–2515.

Massiot, C., McNamara, D.D., Milicich, S.D., Villamor, P., McLean, K., Sepulveda, F., Ries, W.F., Bannister, S.: Fracture permeability in a pervasively fractured rock mass: the role of regional tectonics at Te Mihi, Wairakei Geothermal Field, New Zealand. Proceedings, World Geothermal Congress, Reykjavik, Iceland (2020).

McLean, K., McNamara, D.D.: Fractures interpreted from acoustic formation imaging technology: correlation to permeability. Proceedings, 36th Workshop on Geothermal Reservoir Engineering, Stanford University, Stanford, CA (2011).

McNamara, D.D., Massiot, C., Milicich, S.D.: Characterising the subsurface structure and stress of New Zealand's geothermal fields using borehole images. *Energy Procedia*, 125, (2017), 273-282.

McNamara, D.D, Massiot, C.: Geothermal structural geology in New Zealand: innovative charcterisation and micro-analytical techniques. Proceedings, 38th New Zealand Geothermal Workshop, New Zealand (2016).

McNamara, D.D., Bannister, S., Villamor, P., Sepulveda, F., Milicich, S., Alcaraz, S., Massiot, C.: Exploring structure and stress from depth to surface in the Wairakei Geothermal Field, New Zealand. Proceedings, 41st Workshop on Geothermal Reservoir Engineering, Stanford University, Stanford, CA (2016).

McNamara, D.D., Milicich, S.D., Massiot, C., Villamor, P., McLean, K., Sepulveda, D., Ries, W.F.: Tectonic controls on Taupo Volcanic Zone geothermal expression: insights from Te Mihi, Wairakei Geothermal Field. *Tectonics*, (2019).

McPhie, J., Doyle, M., Allen, R.: Volcanic textures – a guide to the interpretation of textures in volcanic rocks. Centre for Ore Deposit and Exploration Studies, University of Tasmania (1993).

Rider, M.H. The Geological Interpretation of Well Logs, (2nd edition). Cambridge, England. Rider-French Consulting Ltd (1996).

Risk, G.F.: Electrical resistivity survey of the Wairakei geothermal field. Proceedings, 6th New Zealand Geothermal Workshop, Auckland, New Zealand, 123–128 (1984).

Rosenberg, M.D., Bignall, G., Rae, A.J.: The geological framework of the Wairakei–Tauhara geothermal system, New Zealand. *Geothermics*, 38, (2009), 72-84.

Terzaghi, R.D.: Sources of error in joint surveys. *Geotechnique*, 15, (1965), 287–304.

Villamor, P., Clark, K., Watson, M., Rosenberg, M. D., Lukovic, B., Ries, W., González, Á.: New Zealand geothermal power plants as critical facilities: an active fault avoidance study in the Wairakei Geothermal Field, New Zealand. Proceedings, World Geothermal Congress, Melbourne, Australia, 19–25 (2015).

Watton, T.J., Cannon, S., Brown, R.J., Jerram, D.A., Waichel, B.L.: Using formation micro-imaging, wireline logs and onshore analogues to distinguish volcanic lithofacies in boreholes: examples from Palaeogene successions in the Faroe–Shetland Basin, NE Atlantic. *Geological Society, London, Special Publications*, 397, (2014), 173-192.

Wilson, C.J.N., Houghton, B.F., Lloyd, E.F.: Volcanic history and evolution of the Maroa-Taupo area, central North Island. In I.E.M. Smith (ed), Late Cenozoic volcanism in New Zealand. *Royal Society of New Zealand Bulletin*, 23, (1986), 194-223.

Wilson, C.J.N., Houghton, B.F., McWilliams, M.O., Lanphere, M.A., Weaver, S.D., Briggs, R.M.: Volcanic and structural evolution of Taupo Volcanic Zone, New Zealand: a review. *Journal of Volcanology and Geothermal Research*, 68, (1995), 1–28.

Wilson, C.J.N., and Rowland, J.V.: The volcanic, magmatic and tectonic setting of the Taupo Volcanic Zone, New Zealand, reviewed from a geothermal perspective. *Geothermics*, 59, (2016), 1–20.